AMES GRANT

EXPERIMENTAL INVESTIGATION OF HYPERSONIC AERODYNAMICS

IN-02-CR
146991
37 p

Research Report
(Final Report of Principal Investigator Mr. Peter F. Intrieri)

Cooperative Agreement No.: NCC2-475

for the period
April 1, 1987 - June 30, 1988

Submitted to

National Aeronautics and Space Administration
Ames Research Center
Moffett Field, California 94035

Aerothermodynamics Branch
Dr. Gary Chapman, Technical Monitor

Thermosciences Division
Dr. Jim Arnold, Chief

Prepared by

ELORET INSTITUTE
1178 Maraschino Drive
Sunnyvale, CA 94087
Phone: 408 730-8422 or (415) 493-4710
Telex: 15 9201 435
Fax: 408 730-1441
K. Heinemann, President and Grant Administrator
Peter F. Intrieri, Principal Investigator

Summary

An extensive series of ballistic range tests have been conducted at the Ames Research Center to determine precisely the aerodynamic characteristics (particulary drag) of the Galileo entry probe vehicle. Figures and tables are presented herein which summarize the results of these ballistic range tests. Drag data were obtained for both a nonablated and an hypothesized ablated Galileo configuration at Mach numbers from about 0.7 to 14 at Reynolds numbers (based on model diameter) from about 1000 to 4 million. The tests were conducted in air and the experimental results are compared with available Pioneer Venus data since these two configurations are similar in geometry. The nonablated Galileo configuration was also tested with two different center-of-gravity positions to obtain values of pitching-moment-curve slope, C_{m_α}, which could be used in determining values of lift and center-of-pressure location for this configuration. The results indicate that the drag characteristics of the Galileo probe are qualitatively similar to that of Pioneer Venus, however, the drag of the nonablated Galileo is about 3 percent lower (than Pioneer Venus) at the higher Mach numbers and as much as 5 percent greater at transonic Mach numbers of about 1.0 to 1.5. Also, the drag of the hypothesized ablated configuration is about 3 percent lower than that of the nonablated configuration at the higher Mach numbers but about the same at the lower Mach numbers. Additional tests are required at Reynolds numbers of 1000, 500, and 250 to determine if the dramatic rise in drag coefficient measured for Pioneer Venus at these low Reynolds numbers also occurs for Galileo, as might be expected.

Test Facilities

Two ballistic ranges at Ames Research Center are operational and both are being used in the present investigations. The facilities are the Hypervelocity Free Flight Aerodynamic Facility (HFFAF), and the Pressurized Ballistic Range (PBR). These facilities will be described briefly.

Hypervelocity Free Flight Aerodynamic Facility

The test section of the HFFAF is 23 m long and has 16 orthongonal spark shadowgraph stations evenly spaced (1.52 m) over its length. This facility is used primarily for aerodynamic studies. Kerr-cell shutters are used to produce a sharp image of the model and its flow-field on the film. Four deformable-piston, light-gas guns, having bore diameters of 0.71, 1.27, 2.54, and 3.81 cm, are available for launching a model into free flight. Each of these guns can operate to muzzle velocities of about 9 km/sec.

Tests in this facility can be conducted from 1 atm to as low as 20 Hg. The facility has an extremely low leak rate, about 10 Hg per minute. This allows for tests to be conducted in air or in any other nontoxic gas. Tests have been conducted in carbon dioxide, hydrogen, helium, krypton, and xenon.

Pressurized Ballistic Range

The PBR is basically a large tank that can be pressurized or evacuated. It also is used mainly for aerodynamic studies. The test section is 62 m long and has 24 orthogonal spark shadowgraph stations irregularly spaced over its length. The station spacing ranges from 2.1 to 4.2 m. All of the optics are internal to the tank, which imposes a maximum model velocity of

about 3.6 km/sec. At higher velocities, radiation from the gas cap around the model fogs the film, making readings of the model position and attitude impossible. This facility has some advantages over the HFFAF:

1. A much longer model trajectory is obtained (2.7 times).

2. Tests can be conducted above 1 atmosphere, currently to 6 atmos.

3. More detailed shadowgraphs are obtained, primarily because of the simpler internal optics system.

Testing in gases other than air in this facility is impractical because of the large physical volume of the tank.

Galileo Investigations

The ballistic ranges at Ames have supported all of the United States' probe missions to other planets. These include the 1976 Viking Missions to Mars and the 1978 Pioneer Mission to Venus. These facilities are currently being used to support the Galileo Mission to Jupiter. The Galileo spacecraft consists of two major components: The orbitor, which is to orbit Jupiter numerous times while achieving close encounters with many of Jupiter's moons, and a probe, which is to enter and descend through the atmosphere of Jupiter. The probe, scheduled to enter the atmosphere of Jupiter in 1995, will make in situ measurements as it descends through the atmosphere prior to its eventual destruction due to extreme external pressures.

Although some probe aerodynamics were obtained initially in exploratory tests to support early design studies (Ref. 1), more accurate aerodynamics

are needed for support of The Atmosphere Structure Experiment, carried on board the probe.

Atmosphere Structure Experiment

The Atmosphere Structure Experiment is designed to determine the state properties (density, pressure, and temperature) of an unknown planetary atmosphere as functions of altitude from measurements made during the entry and descent of a probe. The experiment consists of a three-axis accelerometer, plus pressure and temperature sensors. After the probe slows down to subsonic Mach numbers, a parachute is deployed and the pressure and temperature sensors can make near-ambient measurements. However, during the high-speed portion of the trajectory, from an entry velocity of 47 km/sec to sonic speed, direct measurements are impractical. The temperature sensor would be burned up and dynamic pressure effects would render the pressure readings useless. The accelerometers alone must yield the state properties during this high-speed phase, and this in turn requires the precise knowledge of the probe aerodynamic characteristics, in particular drag and lift. These characteristics must be known accurately over a wide range of both Mach number and Reynolds number. The ballistic ranges at Ames have proven to be excellent facilities for obtaining this aerodynamic information over wide ranges of Mach number (0.5 - 20) and Reynolds number (250 - 10^7).

Galileo Data

The Galileo probe at entry into the Jovian atmosphere is shown in Fig. 1. It is basically a blunt 45 deg. cone. However, during the high-speed part of the entry, massive ablation takes place. As much as 40% of the vehicle mass at entry is expected to be ablated away, mostly in the nose region, and even the maximum diameter will be significantly decreased. Hence, tests must be conducted not only of the entry configuration but of hypothesized ablated configurations as well.

A sketch of the hypothesized ablated Galileo configuration used in the present tests is shown in Fig. 2 compared with the nonablated configuration. This ablated geometry was derived from heating studies performed in support of the Galileo probe mission by researchers at Ames Research Center, General Electric Company, and others, and is considered to be a reasonable choice for the purpose of the present investigation. (Sensors embedded in the heat shield will help to define the ablated shape during and after the actual entry into Jupiter.)

The models used in the HFFAF tests were homogeneous, machined from either a sintered tungsten alloy (Mallory 3000), steel, aluminum, or polycarbonate plastic (Lexan), which gave a center-of-gravity location $x_{cg}/d = 0.414$ from the nose. Two model sizes were used namely, d = 1.02 cm and 2.03 cm. The models used in the PBR tests were also homogeneous and were machined from brass. These models of the nonablated and ablated configurations had maximum diameters of 5.08 cm and 4.90 cm respectively. The ablated configuration had a center-of-gravity location of $x_{cg}/d = 0.375$ from the nose. Unless specifically stated otherwise, the experimental data presented for Galileo in this report will be for the nonablated configuration (Fig. 1).

A large data bank was available for the Pioneer Venus probe. That configuration was similar to Galileo, as shown in Fig. 3. The nose, corner, and afterbody geometries are all slightly different, but as much use as possible is being made of all Pioneer Venus data to minimize the number of Galileo tests required.

Figure 4 shows some of the Galileo drag data obtained in the present investigation compared with available Pioneer Venus data at the same conditions of velocity and Reynolds number. Open symbols denote Pioneer Venus data and solid symbols are Galileo data. Not surprisingly, the Galileo data are not greatly different from those of Pioneer Venus; the Galileo data are approximately 3 percent lower than the Pioneer Venus data

at the lower angles of attack. However, the differences are real and are important. A 1% error in the knowledge of the probe drag coefficient becomes a 1% error in the density of the atmosphere of Jupiter at that point in the trajectory. This induces a similar error in the derived atmospheric pressure and often errors of many degrees Kelvin in temperature. The success of the Atmosphere Structure Experiment depends on the precise knowledge of the probe aerodynamics which is the driving reason for the many ballistic range tests required.

Ballistic range tests have been conducted for both the nonablated and ablated Galileo configurations to obtain drag data at Mach numbers from about 10 to as low as 0.7. The drag data from these tests are presented in Fig. 5 as a function of Mach number. The Galileo data are the symbols and the line represents a fairing of existing Pioneer Venus drag data in this Mach number range. The open symbols are data obtained in the HFFAF and cover the Mach number range from about 10 to 2.0; the filled symbols are data obtained in the PBR and cover the Mach number range from about 3.5 to 0.7. The drag data obtained at Mach numbers from 2 to 0.7 are required since the probe parachute will not be deployed until the probe slows down to subsonic Mach numbers near 0.8. Since for the most part only one flight was obtained at each Mach number, it was not possible to extrapolate the drag data to obtain values of drag coefficient at zero angle of attack. However, all flights obtained had angles of attack less than 12 degrees and drag coefficient is essentially constant in this angel-of-attack range (see Fig. 4). As stated earlier the flight trajectory for tests in the PBR is much longer than in the HFFAF. Therefore, these flights were divided into 2 or 3 consecutive portions and analyzed separately to give a more detailed definition of C_D vs Mach number, for the same number of flights. This approach is very useful here since large changes in C_D occur with small changes in Mach number below a Mach number of 3.5.

Figure 5 shows that the drag coefficient of the ablated configuration is about 3% less than that of the nonablated configuration at Mach numbers

from 10 to 3.5, but that the drag of both configurations is the same at Mach numbers below 2.5. The variation of drag coefficient with Mach number for Galileo is qualitatively similar to that of Pioneer Venus, however some significant differences are evident, i.e., the drag of the nonablated Galileo is lower by about 3% at a Mach number near 9 but as much as 5% greater at Mach numbers between 1.5 and 1.0. In addition it appears that peak values of C_D for Galileo are reached at a somewhat lower Mach number than for Pioneer Venus. Comparison of the drag data from the two facilities at the same Mach numbers show excellent agreement as expected. The data shown in Fig. 5 for the Mach number range from 0.7 to 1.5 are also presented in Fig. 6 with a greatly expanded Mach number scale. This figure also shows the actual Pioneer Venus data obtained and the fairing used to represent these data.

The nonablated Galileo configuration was also tested with a further-aft center-of gravity location. The primary purpose of these tests was to obtain accurate values of pitching-movement-curve slope which could be used to help determine values of lift and center-of-pressure location for this configuration. (Lift is relatively difficult to obtain accurately in these tests since for this configuration, namely, a 45^{o} half-angle blunted cone at small angles of attack, the lift is very small) As shown in Fig. 7 a bimetallic model was used for these tests. The forebody was constructed of aluminum and the afterbody was machined from phosphor bronze. The two materials were threaded together using a 4-40 screw which was machined integral with the forebody. These bimetallic models had an $x_{cg}/d = 0.476$ compared with 0.414 for the homogeneous models.

The data obtained from these tests and other tests using homogeneous models at a velocity of 3.1 km/sec are presented in Fig. 8 where values of pitching-movement-curve slope, C_{m_α}, are plotted as a function of the root-mean-square resultant angle of attack of each flight. As can be seen there is little effect of angle of attack on C_{m_α} and that the forward cg location gives values about 44% greater than those for the aft cg location.

Although the Reynolds number for these tests are different by a factor of 7, both are sufficiently large to insure similar flow conditions over the models (continuum flow) so that it is not expected that Reynolds number has any significant effect on these data. This difference in Reynolds number resulted because the bimetallic models, being less statically stable, must be tested at a higher static pressure in order to obtain the minimum number of cycles of angular oscillation (1 1/2 to 2 cycles) to yield accurate results.

Ballistic range tests were also conducted to precisely define the drag characteristics of the Galileo probe at a velocity of about 4.6 km/sec at Reynolds numbers (based on model diameter) from about 1 million to as low as about 500. Current plans were to conduct tests at Reynolds numbers of 10^6, 10^5, 10^4, 10^3, 500, and possibly 250, for which Pioneer Venus data exists for direct comparison. The importance of obtaining drag data at these various Reynolds numbers is evident in Fig. 9, which shows Pioneer Venus drag data (for zero angle of attack) down to a Reynolds number of about 250. The drag coefficient increases continuously below a Reynolds number of 1 million, but the increase becomes most dramatic below 1000 where the slip-flow and free-molecule-flow regimes are approached. Earlier ballistic range tests of Pioneer Venus models at Reynolds numbers of 1000 and less proved to be difficult, but techniques were developed which led to successful tests. These same techniques were used in the present low Reynolds number tests conducted in the HFFAF; however, the tests were largely unsuccessful due to the models tumbling or achieving high angles of attack (near 90^0) during the flight, so that no useful drag data could be obtained. This occurs because these tests must be conducted at very low static pressures (approximately 100 to 200 Hg), and any significant angular disturbance imparted to the model upon emergence from the gun muzzle, either by separation from its plastic sabot or by gun blast, cannot be overcome by the low pressure forces acting on the model during flight. The models then pitch up to large angles of attack and even tumble during the flight.

The Galileo data obtained in the present investigations at the various Reynolds numbers are also presented in Fig. 9 and show some anomalies. First, it should be noted that the drag data shown for Galileo at a Reynolds number of 10^6, which agrees closely with that of Pioneer Venus, is for a velocity of 3.4 km/sec (see Fig 4). No additional tests were conducted at 4.6 km/sec since at this relatively high Reynolds number, velocity is not expected to be a strong factor. Several successful Galileo flights were obtained at this higher velocity (4.6 km/sec) at Reynolds numbers of 10^5 and 10^4. Comparison of these data with Pioneer Venus in Fig. 9 shows that the drag for Galileo is about 3 percent lower than for Pioneer Venus at a Reynolds number of 10^5 but nearly 12 percent lower at a Reynolds number of 10^4(flagged symbol) which is considered unlikely. The actual drag data obtained at these two Reynolds numbers from which these values of C_D at $\alpha = 0^o$ were obtained, are presented in Fig. 10, plotted as a function of angle of attack. As can be seen the data at each Reynolds number appear to be entirely consistent with little scatter, however, the large unexpected difference in drag is evident. A probable explanation is that the instrument used to measure static pressure in the test section, developed a slight leak during this series of tests and gave erroneously high readings. An error in pressure of about 0.2 mm Hg out of approximately 2.4 mm Hg (i.e., the nominal pressure desired for these tests) would account for this difference. However, it is surprising that this error must have been essentially the same for each of the five separate tests conducted at this Reynolds number over a period of about a month. This however, must have been the case, since as mentioned earlier, the drag data presented in Fig. 10 show little scatter and extrapolation to $\alpha = 0^o$ is accomplished easily and accurately. Tests by other researchers conducted both immediately prior to and after the above series of Galileo tests, were at one atmosphere of pressure in the test section and so an error in pressure of 0.2 mm Hg would not be discernible in the data. The faulty instrument was replaced and a new system was installed which gave redundant measurements of pressure. A successful flight was obtained at this Reynolds number (10^4) later in the program during another

series of tests designed to obtain Galileo drag data at Reynolds numbers of 1000 and less. As mentioned earlier these tests were largely unsuccessful. This one flight (no. 1766) unfortunately achieved relatively high angles of attack and so the drag coefficient obtained and shown in Fig. 9 is for an angle of attack of 19.6 degrees. An approximate extrapolation of this one data point to $\alpha = 0^{o}$ was accomplished using the variation of C_D versus angle of attack obtained for Pioneer Venus at the same test conditions. This procedure gave a value of C_D of 1.06 for this Reynolds number, which as can be seen in Fig. 9, is again only about 3 percent less than that of Pioneer Venus.

No successful Galileo flights were obtained at a Reynolds number of 500, and only one successful flight was obtained at a Reynolds number of 1000. This flight (no. 1762) also achieved higher than desired angles of attack and the value of C_D shown in Fig. 9 is for an angle of attack of 14.7 degrees. Extrapolation to $\alpha = 0^{o}$ was accomplished, again using existing Pioneer Venus data at the same test conditions, in the same manner as just described for flight no. 1766. However, in this case the resulting value of C_D of 1.06 is seen to be far below the value obtained for Pioneer Venus at this Reynolds number. It is believed that no firm conclusions should be made here on the basis of only this one flight. Additional tests are required at Reynolds numbers of 1000, 500, and 250 to determine reliably if the dramatic rise in drag coefficient measured for Pioneer Venus at these low Reynolds numbers also occurs for Galileo, as might be expected.

Reference

1. Intrieri, P.F. and Kirk, D.B.: High-Speed Aerodynamics of Several Blunt-Cone Configurations. Journal of Spacecraft and Rockets, Volume 24, No. 2, pp. 127-132, March-April 1987.

List of Tables

List of Figures

SUMMARY - GALILEO ENTRY PROBE DATA

Table I - Aerodynamic Data

	1	2	3	4	5	6	7	8	9	10	11	12	13	14
	Test no.	V_{avg} ft/sec	Re_d $\times 10^6$	M	Pressure mm Hg	← config.	Model d(nom) inches	mat'l →	α_{rms} deg.	C_D	C_{m_α}	C_{L_α}	Facility	
1	1629	9895	4.03	8.74	766.2	nonabl.	0.80	mallory	2.39	1.0337			HEFAF	
2	1630	9903	4.06	8.76	768.2	↓	↓	↓	4.71	1.0304			↓	
3	1631	10156	4.16	9.00	760.9	↓	↓	↓	2.07	1.0404			↓	
4														
5	1633	10128	.100	8.96	18.62	↓	0.80	mallory	13.40	.9792			↓	
6	1634	10331	.102	9.12	18.60	↓	↓	↓	11.02	.9892			↓	
7	1635	10515	.106	9.28	19.05	↓	↓	↓	7.33	1.0323			↓	
8														
9	1697	8300	.082	7.31	37.68	↓	0.40	steel	4.92	1.0336	-.169	-.167	↓	
10	1698	10624	.106	9.39	37.72	↓	↓	↓	3.95	1.0488	-.174	-.138	↓	
11	1699	10402	.104	9.18	37.71	↓	↓	↓	2.05	1.0205	-.169	-.137	↓	
12														
13	1675	12415	.858	10.93	130.20	↓	0.80	AL/PB	1.87	1.0034	-.123	-.157	↓	
14	1676	11486	.798	10.15	130.60	↓	↓	↓	4.45	1.0152	-.119	-.030	↓	
15	1679	9533	.650	8.39	130.00	↓	↓	↓	9.29	1.0185	-.113	+.014	↓	
16	1687	10432	.732	9.23	131.50	↓	↓	↓	4.22	1.0103	-.114	+.037	↓	
17	1689	10893	.762	9.66	130.00	↓	↓	↓	16.82	1.0018	-.110	-.029	↓	
18														
19	1644	6971	2.81	6.17	756.0	↓	0.80	mallory	9.64	1.0699			↓	
20	1645	4412	1.77	3.90	756.4	↓	↓	↓	5.35	1.1415			↓	
21	1648	2776	1.11	2.45	753.2	↓	↓	↓	6.30	1.2776			↓	
22	1652	2525	1.02	2.23	763.5	↓	↓	↓	4.73	1.2772			↓	
23														
24	1683	6774	2.62	5.97	762.0	ablated	0.773	mallory	3.27	1.0355	-.188	-.352	↓	
25	1684	4160	1.63	3.67	765.2	↓	↓	↓	3.28	1.1119	—	—	↓	
26	1685	2060	0.81	1.82	763.2	↓	↓	↓	8.18	1.2627	-.090	-.488	↓	
27	1686	10995	4.30	9.70	763.0	↓	↓	↓	2.89	1.0166	-.198	-.398	↓	
28														
29														
30														

SUMMARY - GALILEO ENTRY PROBE DATA

Table I - Aerodynamic Data - continued

	1	2	3	4	5	6	7	8	9	10	11	12	13	14
	Test no.	V_{avg} ft/sec	Re_d	M	Pressure mm Hg	← config.	Model d(nom) inches	mat'l →	α_{rms} deg.	C_D	C_{m_α}	C_{L_α}	Facility	
1	1655	15111	1.00×10^4	13.45	2.44	nonabl.	0.40	Alum	3.70	.9394			HFFAF	
2	1656	14870	0.98	13.23	2.42				12.91	.8302				
3	1659	15414	0.96	13.55	2.39				11.11	.9191				
4	1660	16116	1.00	14.16	2.40				4.94	.9122				
5	1661	15270	0.95	13.38	2.41				8.96	.9092				
6	1766	15705	0.97	13.86	2.44			Lexan	19.24	.9861				
7														
8	1691	14704	0.94×10^5	12.87	24.95		0.40	steel	1.91	1.0320	-.292	—		
9	1693	15515	0.94	12.72	25.12				3.09	1.0284	-.184	—		
10	1695	14839	0.95	12.99	25.00				2.37	1.0259	-.196	—		
11	1696	14663	0.94	12.82	25.20				3.92	1.0073	-.154	—		
12														
13	1762	16629	1.09×10^3	14.61	0.264	nonabl.	0.40	Lexan	14.68	1.0249	—	—	HFFAF	
14														
15														
16														
17														
18														
19														
20														
21														
22														
23														
24														
25														
26														
27														
28														
29														
30														

SUMMARY - GALILEO ENTRY PROBE DATA

Table I - Aerodynamic Data - continued

	1	2	3	4	5	6	7	8	9	10	11	12	13	14
	Test no.	V_{avg} ft/sec	Re_d $\times 10^6$	M	Pressure mm Hg	← config.	Model d(nom) inches	mat'l →	α_{rms} deg.	C_D	$C_{m\alpha}$	$C_{L\alpha}$	Facility	Station interval
1	1845	1511	1.57	1.35	764.5	nonabl.	2.00	Brass	4.88	1.2925	-.0868	-.873	PBR	1-17
2	↓	1582	1.65	1.41	↓	↓	↓	↓	2.80	1.3024	-.0814	-.863	↓	1-10
3	↓	1427	1.49	1.27	↓	↓	↓	↓	6.48	1.2732	-.0843	-.908	↓	9-17
4														
5	1846	1462	1.55	1.31	764.6	↓	↓	↓	5.43	1.2814	-.0851	-.850	↓	1-17
6	↓	1530	1.62	1.37	↓	↓	↓	↓	3.89	1.2970	-.0864	-.842	↓	1-10
7	↓	1381	1.46	1.23	↓	↓	↓	↓	6.90	1.2587	-.0813	-.852	↓	9-17
8														
9	1849	961	1.01	0.86	765.8	↓	↓	↓	1.58	.9217	-.1102	-.378	↓	1-17
10	↓	993	1.05	0.89	↓	↓	↓	↓	1.46	.9440	-.1115	-.432	↓	1-10
11	↓	922	.97	0.82	↓	↓	↓	↓	1.72	.8942	-.1043	-.336	↓	9-17
12														
13	1851	1132	1.19	1.01	761.3	↓	↓	↓	3.99	1.1686	-.1069	-.631	↓	1-17
14	↓	1180	1.24	1.05	↓	↓	↓	↓	3.10	1.2257	-.1072	-.734	↓	1-10
15	↓	1075	1.13	0.96	↓	↓	↓	↓	5.01	1.0659	-.1047	-.582	↓	9-17
16														
17	1869	2543	2.63	2.26	758.2	↓	↓	↓	2.99	1.2878	-.0655	-.655	↓	1-17
18	↓	2660	2.75	2.37	↓	↓	↓	↓	2.57	1.2685	-.0612	-.669	↓	1-10
19	↓	2402	2.49	2.14	↓	↓	↓	↓	3.22	1.2929	-.0674	-.814	↓	9-17
20														
21														
22														
23														
24														
25														
26														
27														
28														
29														
30														

SUMMARY - GALILEO ENTRY PROBE DATA

Table I - Aerodynamic Data - concluded

	1	2	3	4	5	6	7	8	9	10	11	12	13	14
	Test no.	V_{avg} ft/sec	Re_d $\times 10^6$	M	Pressure mm Hg	config.	Model d(nom) inches	mat'l	α_{rms} deg.	C_D	C_{m_α}	C_{L_α}	Facility	Station interval
1	1847	1549	1.61	1.39	766.8	ablated	1.930	Brass	4.57	1.2881	-.0948	-.858	PBR	1-17
2	↓	1625	1.69	1.46	↓	↓	↓	↓	3.20	1.2894	-.1962	-1.002	↓	1-10
3	↓	1458	1.52	1.31	↓	↓	↓	↓	5.32	1.2740	-.0858	-.824	↓	9-17
4														
5	1850	852	.87	.76	761.0	↓	↓	↓						
6	↓	878	.90	.79	↓	↓	↓	↓	5.63	.8374	-.1018	-.302	↓	1-17
7	↓	819	.84	.73	↓	↓	↓	↓	5.67	.8341	-.0994	-.292	↓	1-10
8									5.88	.8332	-.1034	-.316	↓	9-17
9	1853	1651	1.66	1.47	760.0	↓	↓	↓						
10	↓				↓	↓	↓	↓	4.39	1.2922	-.0368	-.809	↓	1-17
11	↓				↓	↓	↓	↓		1.2944	—	—	↓	1-10
12										1.2761	—	—	↓	9-17
13	1854	1227	1.22	1.09	761.5	↓	↓	↓						
14	↓	1283	1.28	1.14	↓	↓	↓	↓	5.17	1.2291	-.1064	-.806	↓	1-17
15	↓	1160	1.16	1.03	↓	↓	↓	↓	3.41	1.2431	-.1079	-.885	↓	1-10
16									6.75	1.2249	-.1006	-.769	↓	9-17
17	1870	2332	2.34	2.08	760.8	↓	↓	↓						
18	↓	2444	2.45	2.18	↓	↓	↓	↓	.92	1.2862	-.0564	-.557	↓	1-17
19	↓	2197	2.20	1.96	↓	↓	↓	↓	.91	1.2750	—	—	↓	1-10
20									.92	1.2887	—	—	↓	9-17
21	1877	3818	3.65	3.36	758.2	↓	↓	↓						
22	↓	3975	3.80	3.50	↓	↓	↓	↓	1.85	1.1412	-.1854	-.120	↓	1-17
23	↓	3598	3.44	3.16	↓	↓	↓	↓	1.93	1.1120	-.1794	+.015	↓	1-10
24									1.89	1.1521	-.1852	+.097	↓	9-17
25														
26														
27														
28														
29														
30														

SUMMARY - GALILEO ENTRY PROBE DATA

Table II - Model Physical Characteristics

	1	2	3	4	5	6	7	8	9	10	11	12	13	14
	Test no.	config.	mat'l.	weight gm.	max. dia. inches	$\frac{x_{cg_{nose}}}{d}$	I_y slug-ft^2	$\frac{I_y}{I_x}$						
1	1629	nonabl.	mallory	36.8240	.8001	.414	6.83×10^{-7}	.7610						
2	1630			36.5715	.8005		6.77	.7577						
3	1631			36.6300	.8003		6.80	.7588						
4														
5	1633			36.5862	.8003		6.80	.7597						
6	1634			36.6565	.8002		6.83	.7623						
7	1635			36.5965	.8002		6.80	.7617						
8														
9	1697		steel	2.0949	.4000		9.89×10^{-9}	.7607						
10	1698			2.0730	.3997									
11	1699			2.0859	.4002									
12														
13	1675		AL/PB	9.3435	.8000	.475	1.65×10^{-7}	.7804						
14	1676			9.3538	.8000	.476								
15	1679			9.3390	.8000	.475								
16	1687			9.3665	.8000	.476								
17	1689			9.3082	.8000	.476								
18														
19	1644		mallory	36.5990	.8002	.414	6.81×10^{-7}	.7626						
20	1645			36.6353	.8001		6.80	.7591						
21	1648			36.5633	.8002		6.78	.7599						
22	1652			36.7463	.8001		6.82	.7600						
23														
24	1683	ablated		32.8082	.7730	.375	5.62×10^{-7}	.7566						
25	1684			32.9530	.7730	.374	5.65	.7557						
26	1685			32.7373	.7730	.373	5.64	.7582						
27	1686			32.3810	.7731	.375	5.55	.7530						
28														
29														
30														

SUMMARY - GALILEO ENTRY PROBE DATA

Table II - Model Physical Characteristics - continued

	1	2	3	4	5	6	7	8	9	10	11	12	13	14
	Test no.	config.	mat'l,	weight gm.	max. dia. inches	$\frac{x_{cg_{nose}}}{d}$	I_y slug-ft^2	$\frac{I_y}{I_x}$						
1	1655	nonabl	alum.	.7640	.4004	.414	3.53×10^{-9}	.7607						
2	1656			.7592	.4003									
3	1659			.7615	.4000									
4	1660			.7601	.3998									
5	1661		↓	.7628	.4001		↓							
6	1766		lexan	.3181	.3983		1.51×10^{-9}							
7														
8	1691		Steel	2.1197	.4008		9.89×10^{-9}							
9	1693			2.1184	.4009									
10	1695			2.0853	.4002									
11	1696		↓	2.0742	.3997		↓							
12														
13	1762	↓	lexan	.3199	.3986	↓	1.51×10^{-9}	↓						
14														
15														
16														
17														
18														
19														
20														
21														
22														
23														
24														
25														
26														
27														
28														
29														
30														

SUMMARY - GALILEO ENTRY PROBE DATA

Table II - Model Physical Characteristics - concluded

	1	2	3	4	5	6	7	8	9	10	11	12	13	14
	Test no.	config.	mat'l.	weight gm.	max. dia. inches	$\frac{x_{cg_{nose}}}{d}$	I_y slug-ft^2	$\frac{I_y}{I_x}$						
1	1845	nonabl.	brass	280.02	2.000	.414	3.20×10^{-5}	.7512						
2														
3	1846			280.49	2.000		3.21×10^{-5}	.7499						
4														
5	1849			279.85	2.000		3.20×10^{-5}	.7512						
6														
7	1851			279.85	2.000		3.20×10^{-5}	.7512						
8														
9	1869	↓		279.60	2.000	↓	3.20×10^{-5}	.7512						
10														
11	1847	ablated		251.24	1.930	.373	2.65×10^{-5}	.7383						
12														
13	1850			251.10	1.930		2.65×10^{-5}	.7383						
14														
15	1853			251.10	1.930		2.65×10^{-5}	.7383						
16														
17	1854			250.92	1.930		2.65×10^{-5}	.7383						
18														
19	1870			250.89	1.930		2.65×10^{-5}	.7383						
20														
21	1877	↓	↓	250.69	1.930	↓	2.65×10^{-5}	.7383						
22														
23														
24														
25														
26														
27														
28														
29														
30														

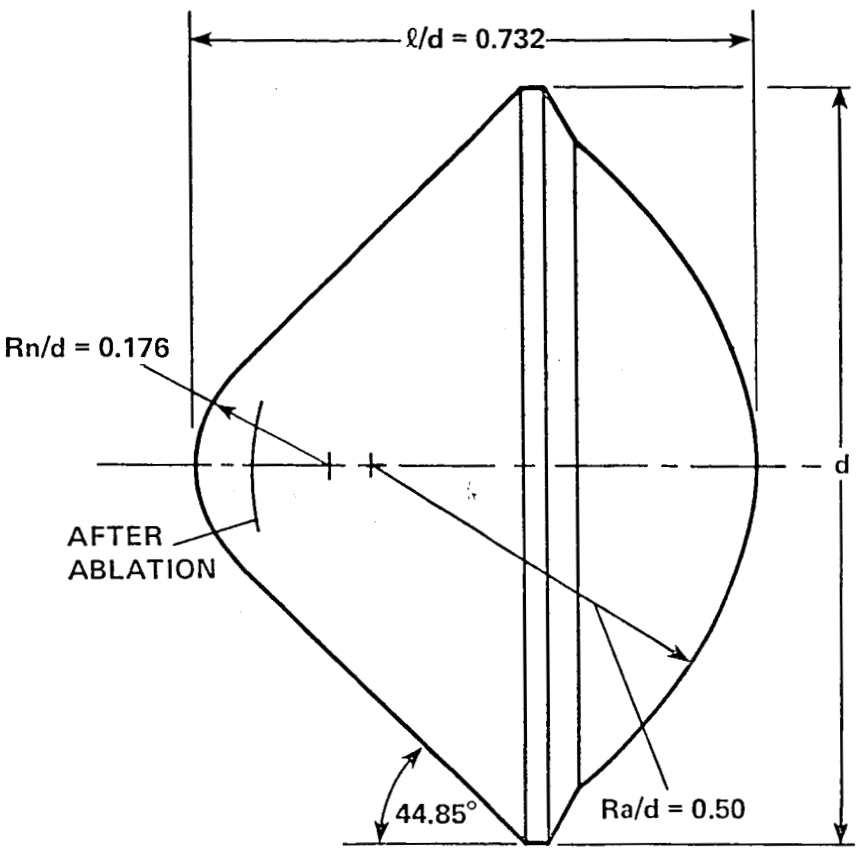

Figure 1.- Galileo Entry Probe Configuration.

Ablated Galileo forebody coordinates
dimensions in inches

X	Y
0	0
0.002	0.936
.057	1.913
.192	2.957
.378	4.142
.550	4.787
1.020	5.706
1.513	6.451
2.853	8.208
4.326	9.830
7.365	12.981
10.468	16.068
13.612	19.113
16.785	22.130
18.792	24.028

r (full scale) = 24.900 inches (0.632 m)

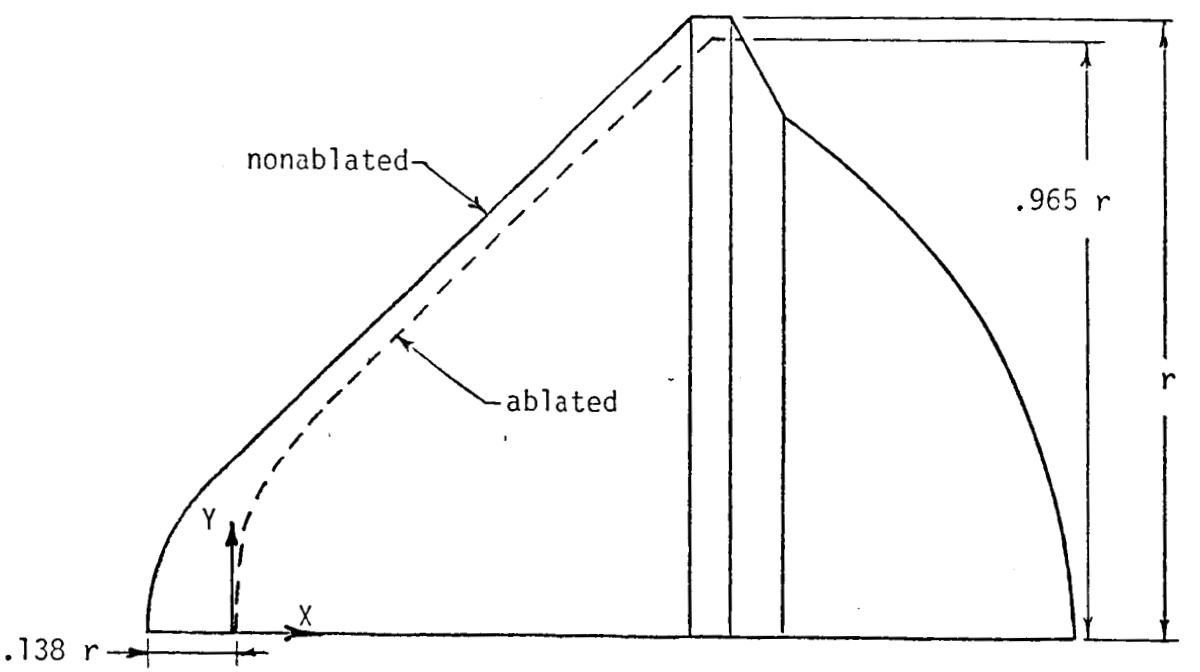

Figure 2.- Comparison of Galileo nonablated and ablated geometries.

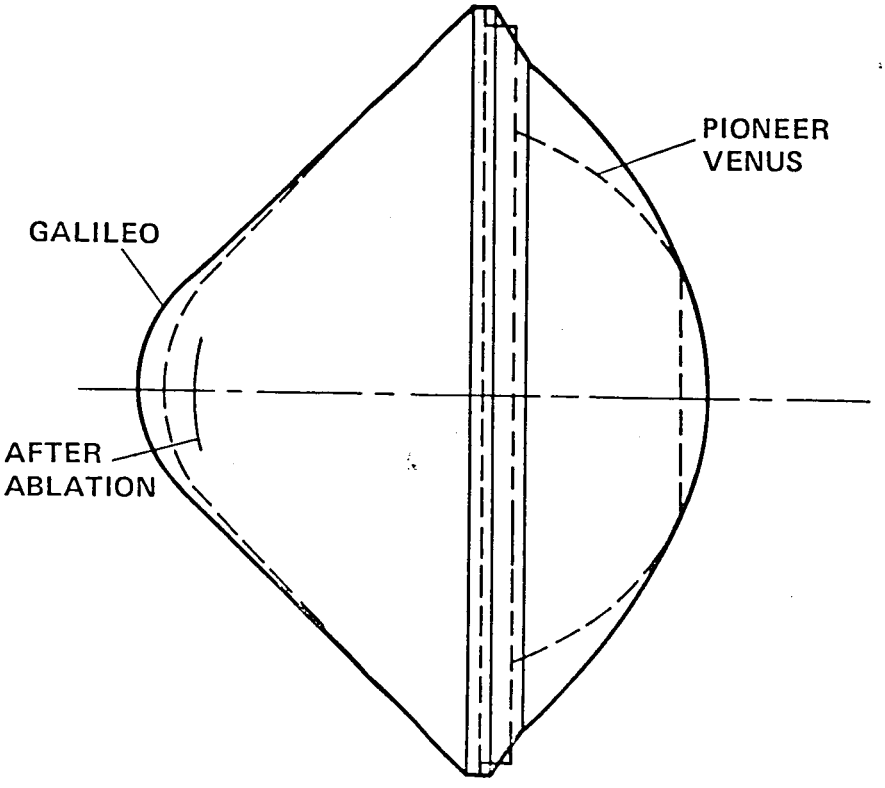

Figure 3.- Comparison of Galileo and Pioneer Venus geometries.

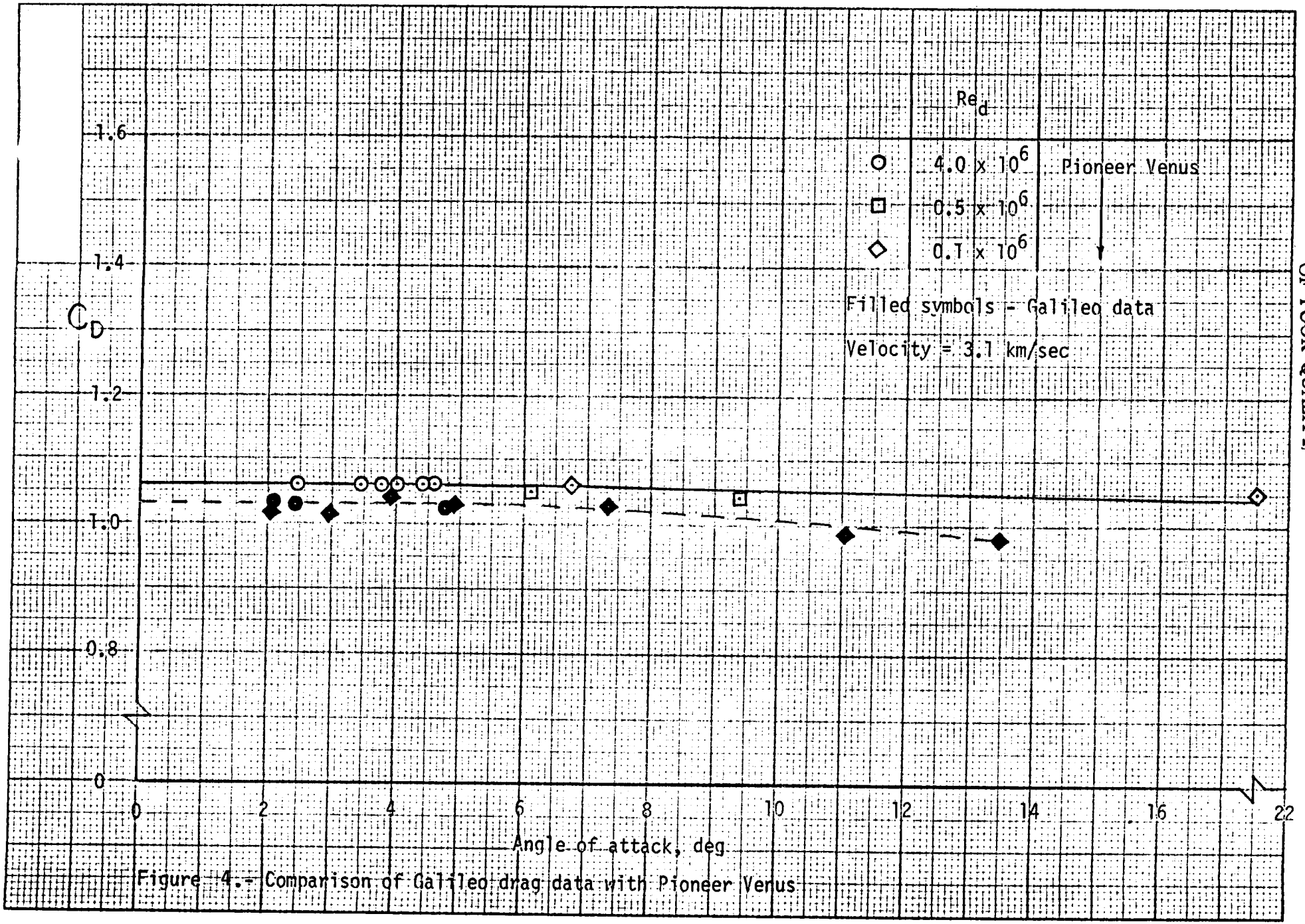

Figure 4.- Comparison of Galileo drag data with Pioneer Venus

Figure 5.- Variation of drag coefficient with Mach number for Galileo and Pioneer Venus.

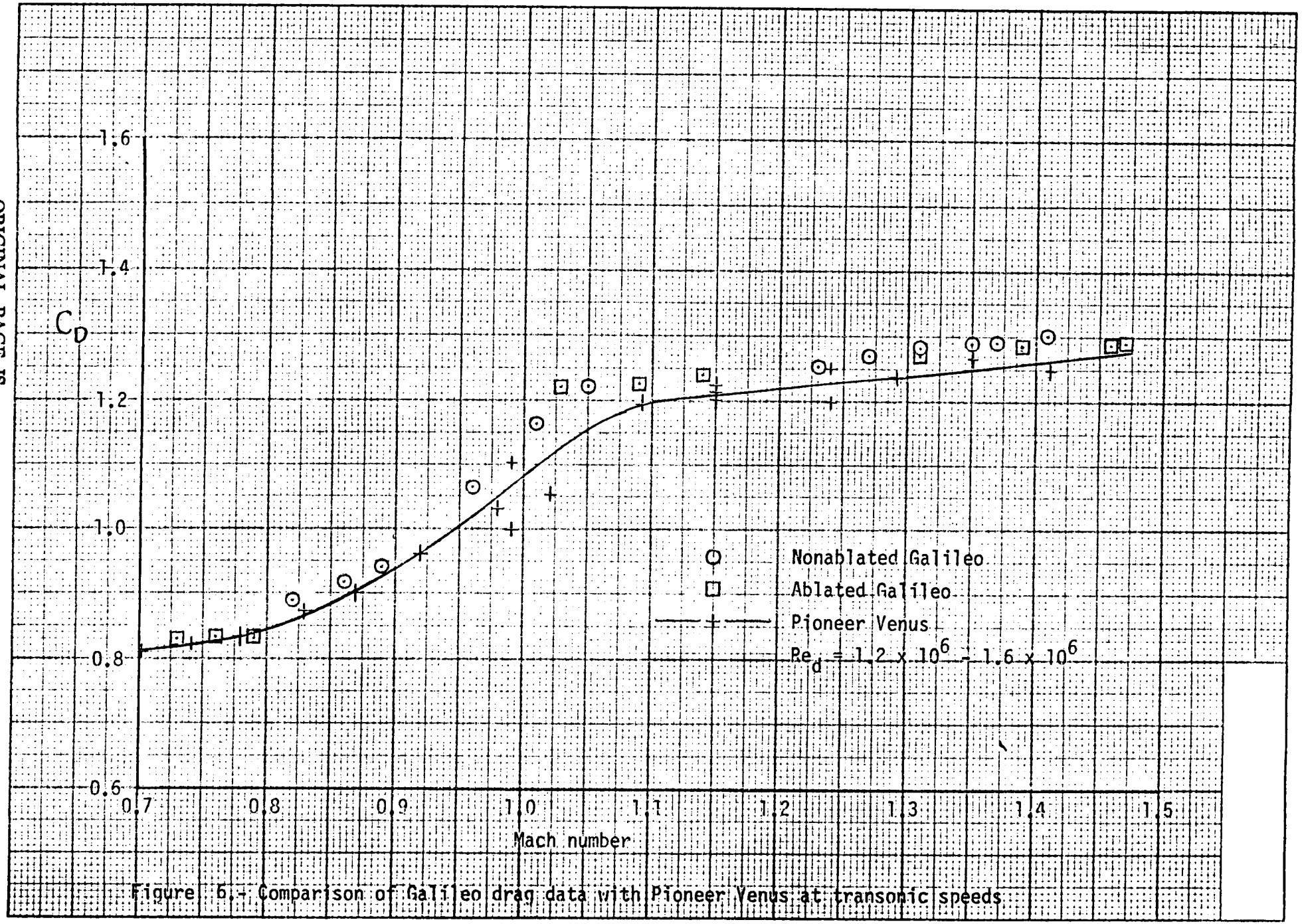

Figure 6.- Comparison of Galileo drag data with Pioneer Venus at transonic speeds

ORIGINAL PAGE IS
OF POOR QUALITY

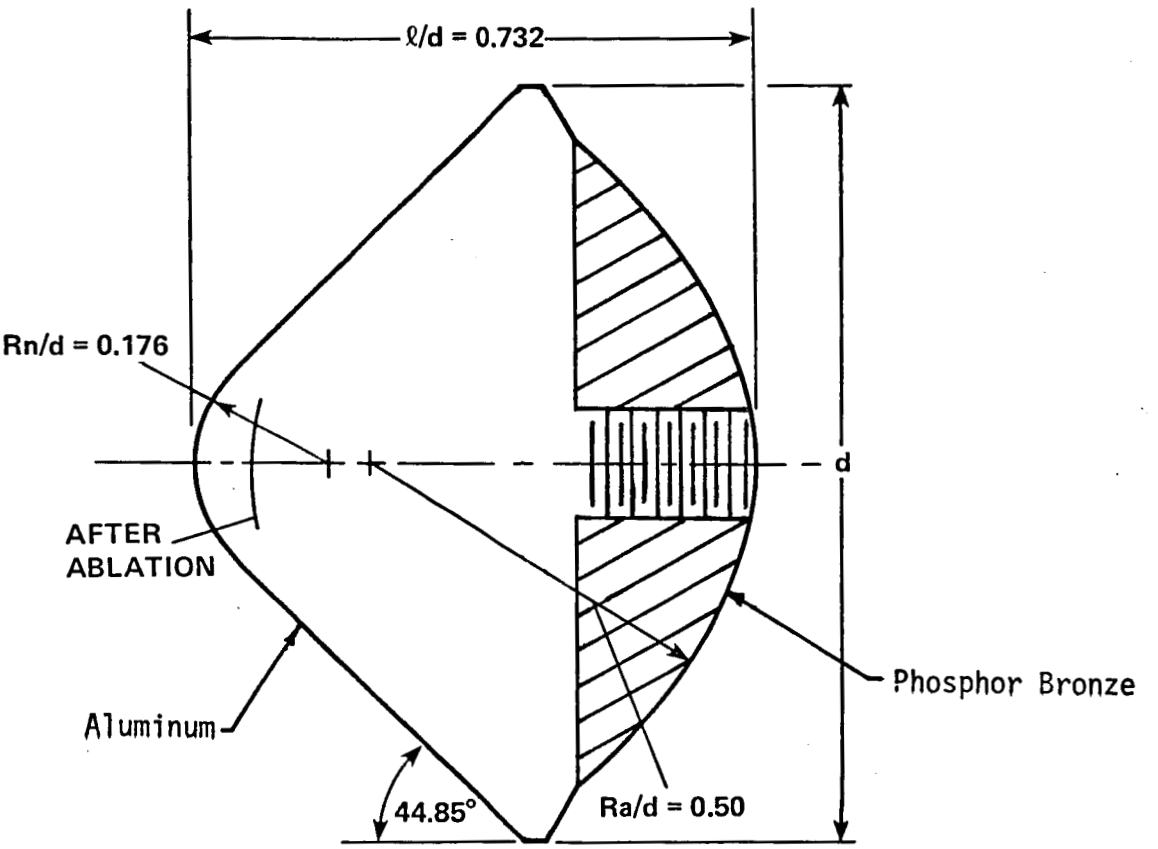

Figure 7.- Galileo Entry Probe Configuration, bimetallic model, $X_{cg}/d = 0.476$.

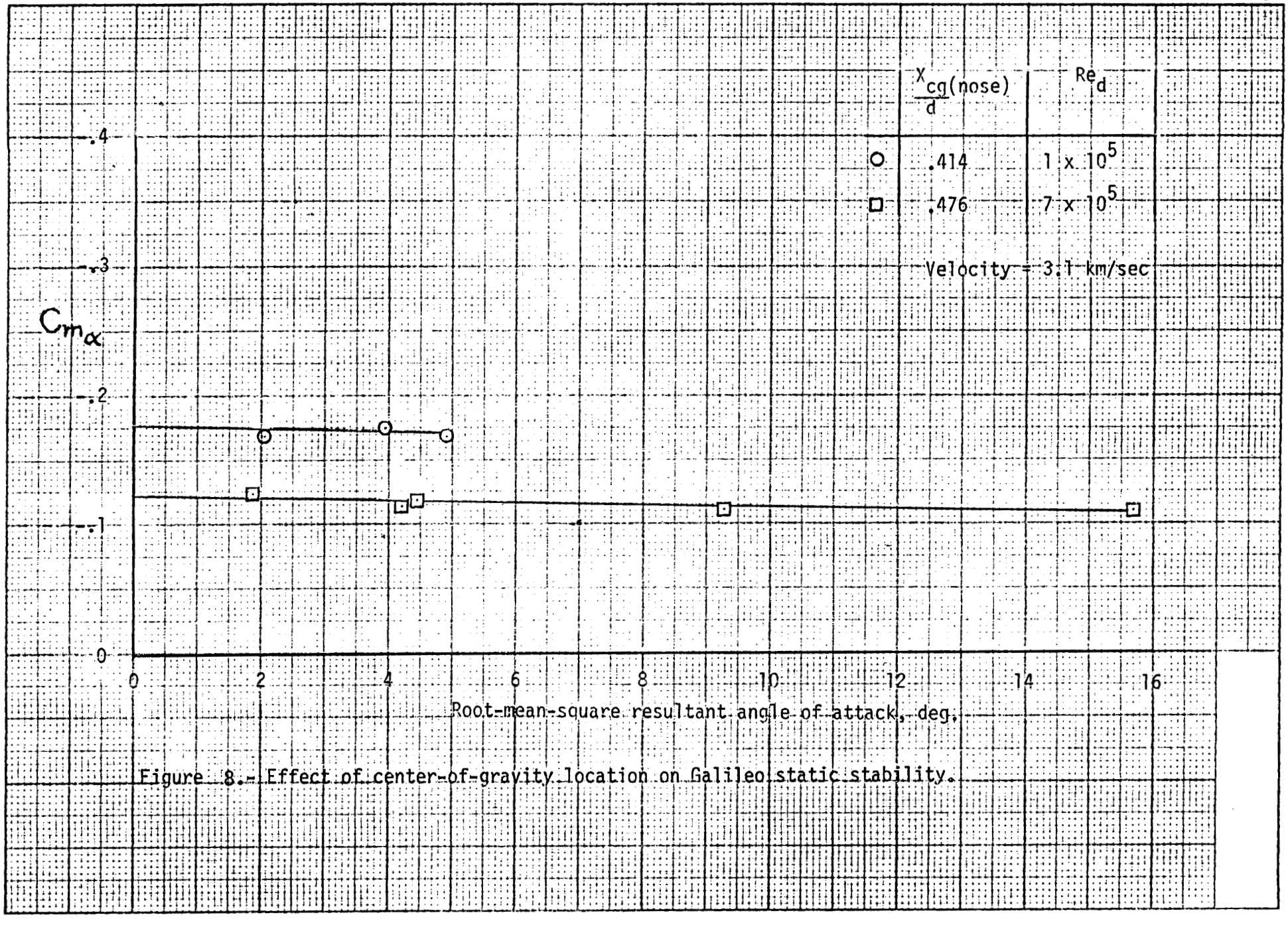

Figure 8.- Effect of center-of-gravity location on Galileo static stability.

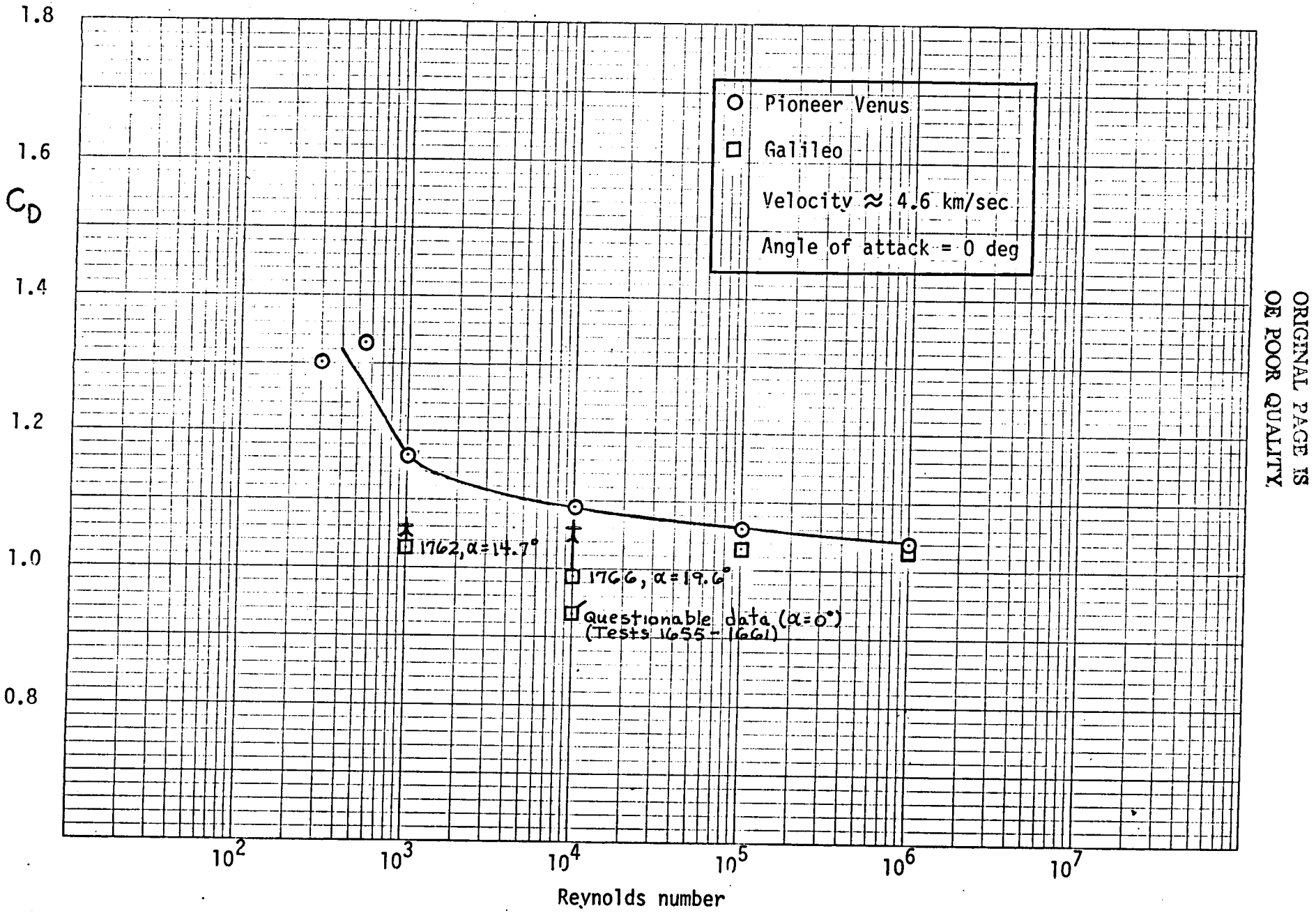

Figure 9. - Effect of Reynolds number on drag characteristics of Galileo and Pioneer Venus probe vehicles.

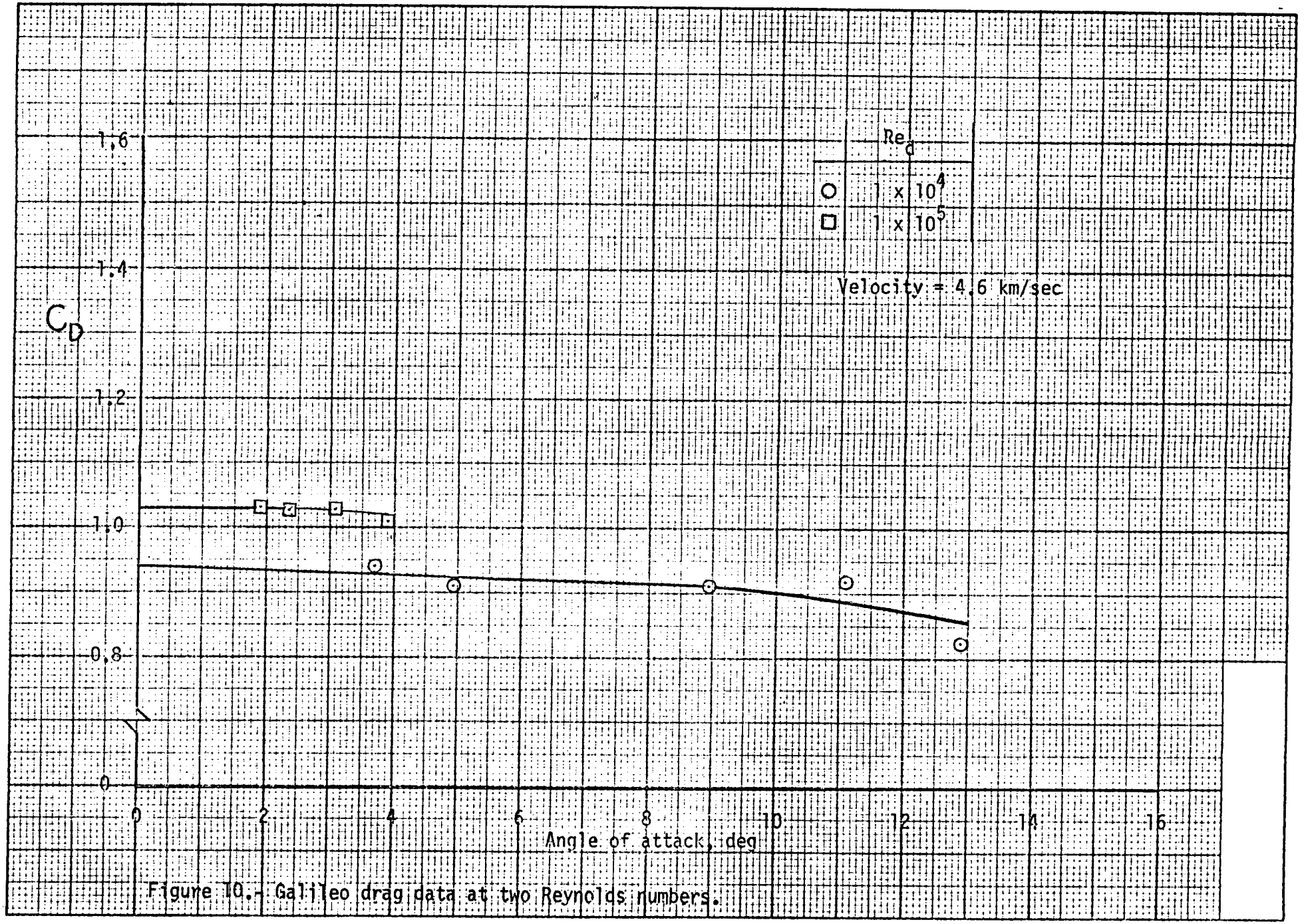

Figure 10.- Galileo drag data at two Reynolds numbers.

Low Reynolds number sphere drag data
and additional relevant figures

SPHERE DRAG DATA

	1	2	3	4	5	6	7	8	9	10	11	12	13	14
	Test no.	V_{avg} ft/sec	Re_d	M	Test gas	Pressure mm Hg	config.	Model dia. inches	mat'l	C_D	Facility	Model Wt gm		
1	1359	12931	198	14.5	87% CO_2 13% Air	.067	Sphere	.190	nylon	1.831	HFFAF	.0660		
2	1360	13144	206	11.6	Air	.124	↓	.189	↓	1.617	↓	.0660		
3	1361	12891	192	14.4	CO_2	.066	↓	.189	↓	1.806	↓	.0662		
4	1374	13225	4564	15.1	CO_2	1.440	↓	.189	↓	1.053	↓	.0660		
5														
6														
7														
8														
9														
10														
11														
12														
13														
14														
15														
16														
17														
18														
19														
20														
21														
22														
23														
24														
25														
26														
27														
28														
29														
30														

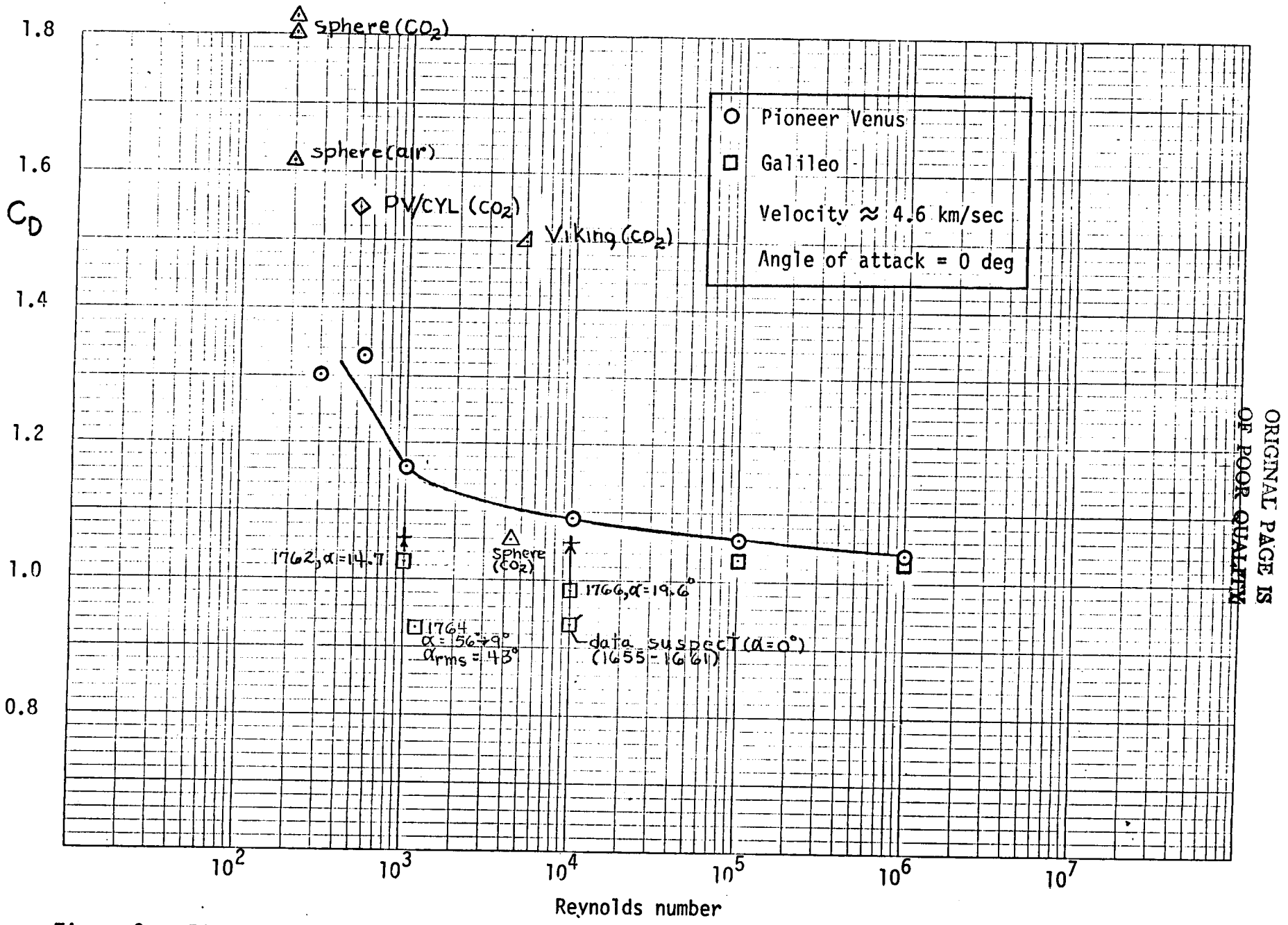

Figure 9a.- Effect of Reynolds number on drag characteristics of Galileo and Pioneer Venus probe vehicles.

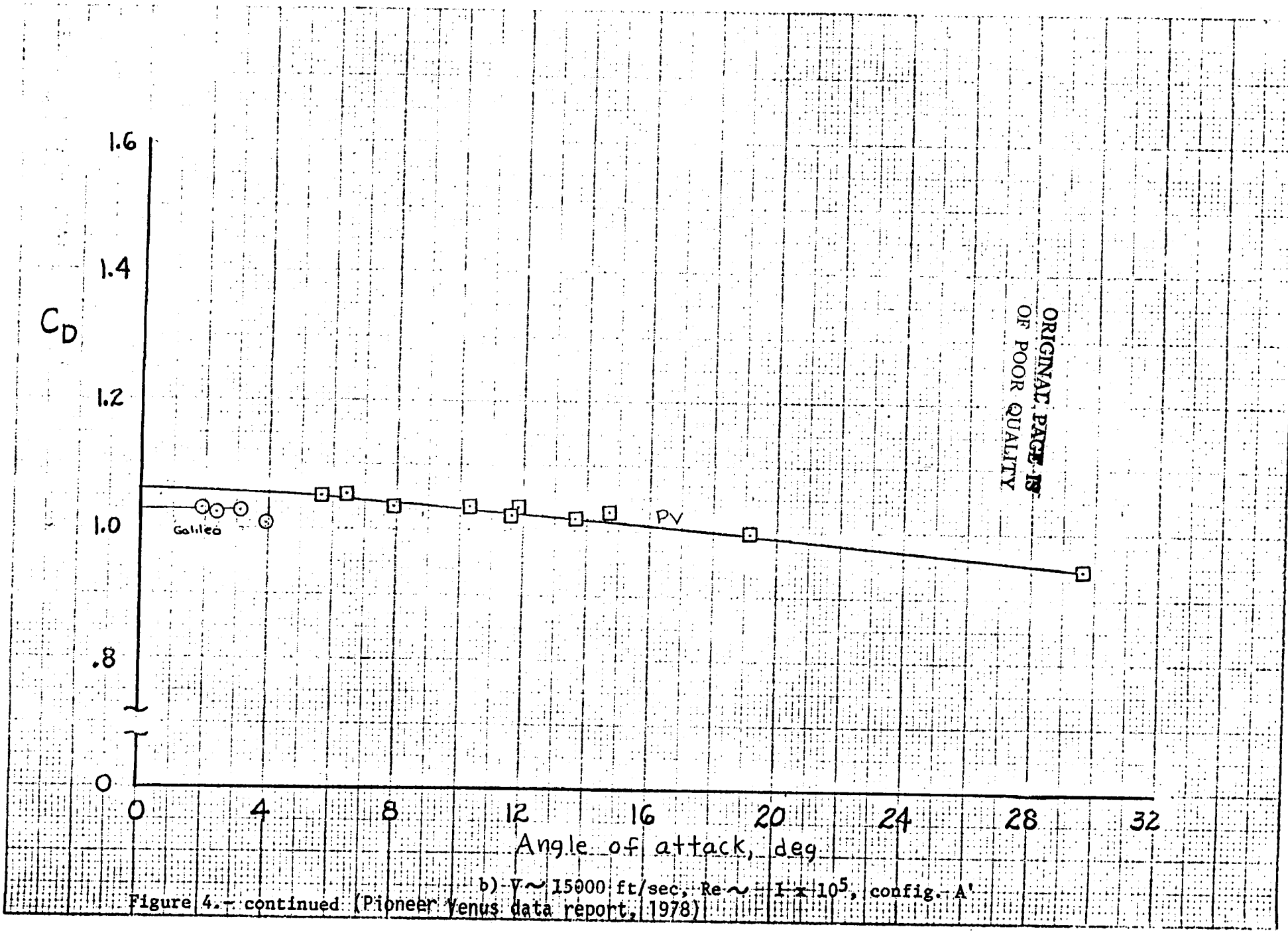

b) V ~ 15000 ft/sec, Re ~ 1 x 10^5, config. A'

Figure 4.- continued (Pioneer Venus data report, 1978)

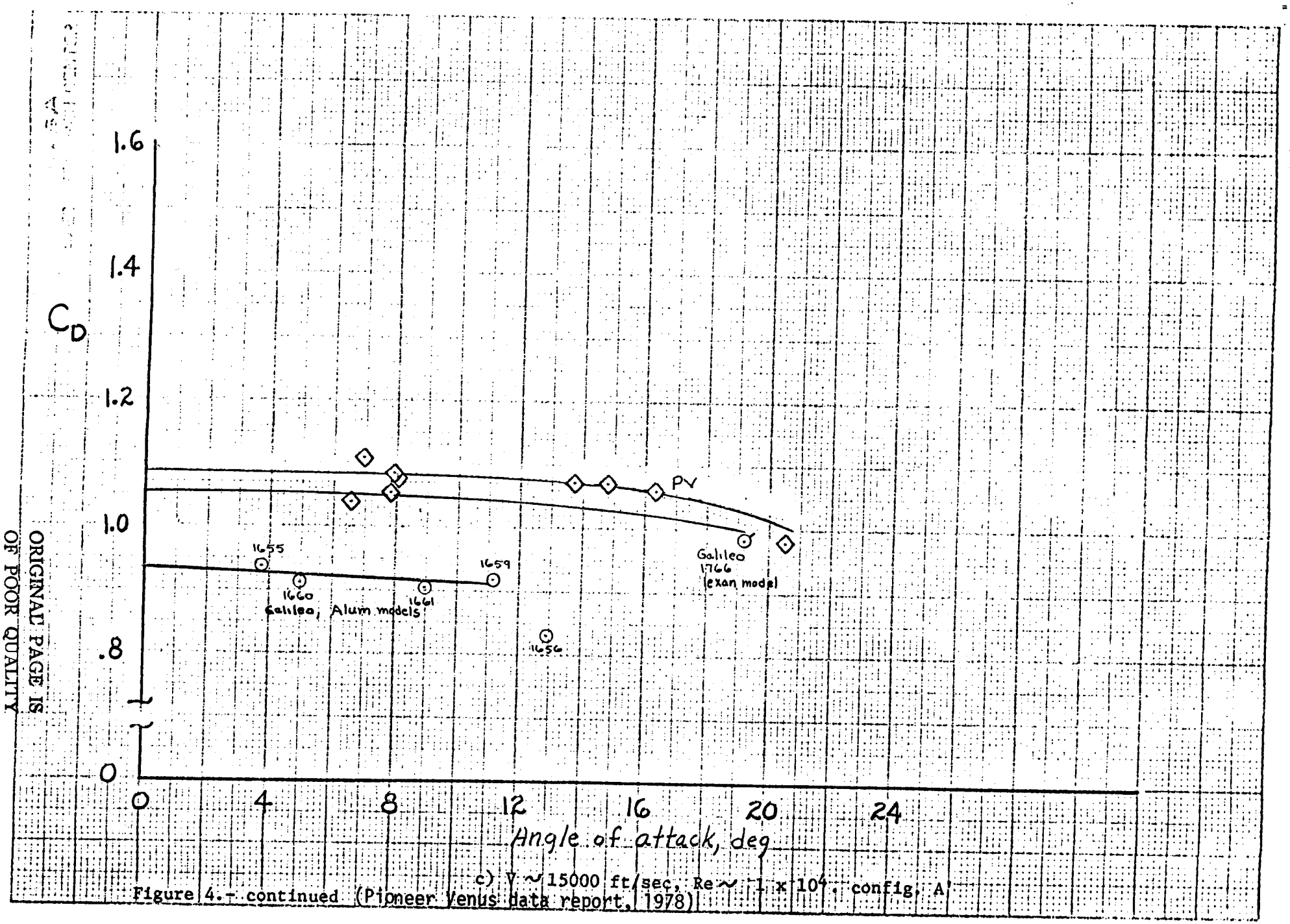

c) V ~ 15000 ft/sec, Re ~ 1 x 10^4, config. A'

Figure 4.- continued (Pioneer Venus data report, 1978)

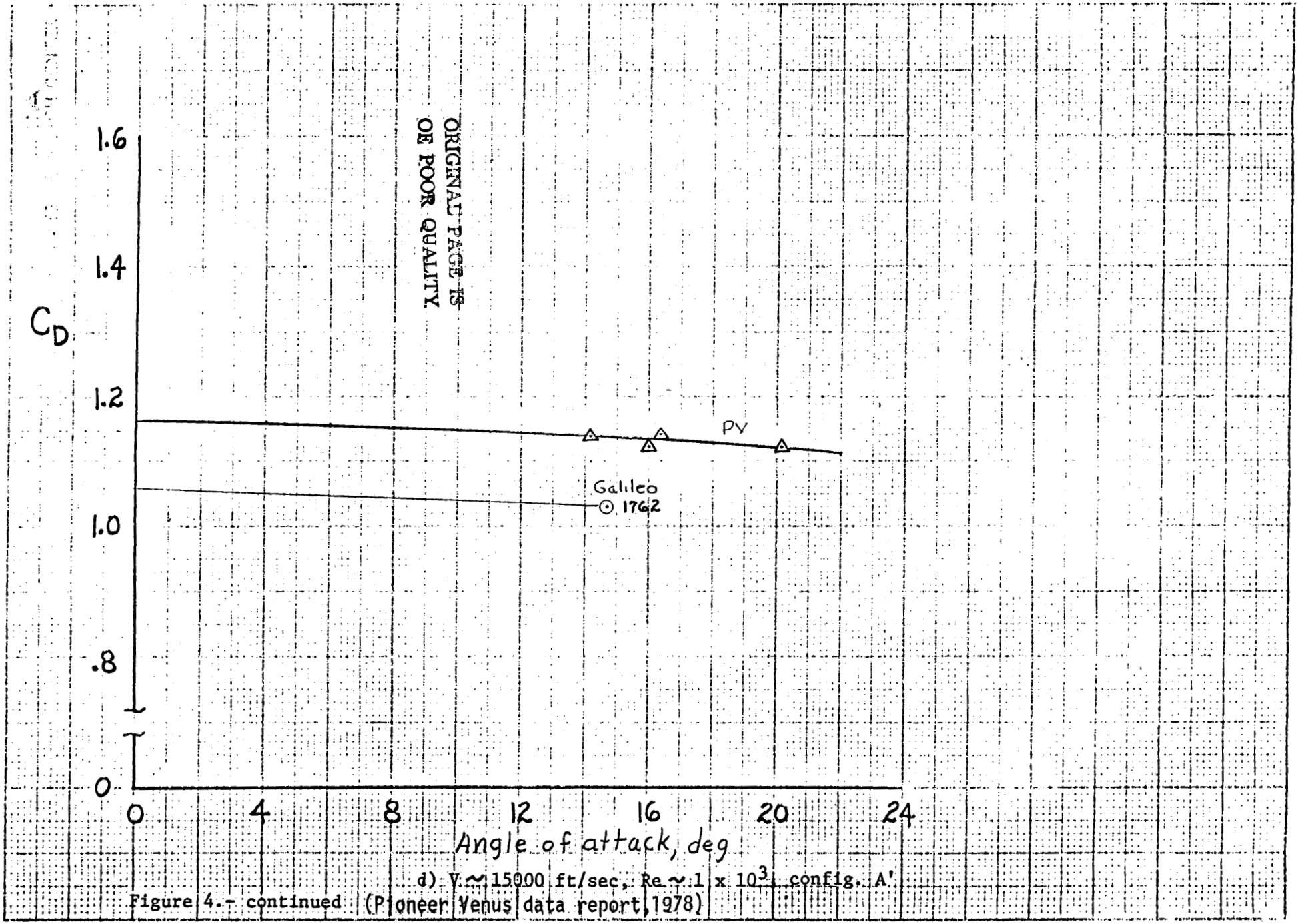

d) V ~ 15000 ft/sec, Re ~ 1 x 10^3, config. A'

Figure 4.- continued (Pioneer Venus data report, 1978)